Sixteen years of X-ray monitoring of Sagittarius A*: Evidence for a decay of the faint flaring rate from 2013 August, 13 months before a rise in the bright flaring rate

Enmanuelle Mossoux and Nicolas Grosso

Observatoire astronomique de Strasbourg, CNRS, Université de Strasbourg, UMR 7550, 11 rue de l'Université, F-67000 Strasbourg, France; emossoux@ulg.ac.be

Observatoire astronomique de Strasbourg

UNIVERSITÉ DE STRASBOURG

PNHE Programme national hautes énergies

This poster Mossoux et al. (2017)

THE X-RAY UNIVERSE 2017

xmm-newton

Abstract

Thanks to the overall 1999-2015 Chandra, XMM-Newton and Swift observations of the supermassive black hole at the center of our Galaxy, Sgr A*, we tested the significance and persistence of the increase of "bright and very bright" X-ray flaring rate argued by Ponti et al. (2015, MNRAS, 454, 1525) who studied the 1999–2014 Chandra and XMM-Newton public observations and the 2014 Swift monitoring. We detected the flares observed with Swift using the binned light curves whereas those observed by XMM-Newton and Chandra were detected using the two-steps Bayesian blocks algorithm with a prior number of change points properly calibrated and a false positive rate for the flare detection of 0.1% (Mossoux, et al. 2015, A&A, 573, A46). We then applied this algorithm on the flare arrival times corrected from the detection efficiency computed for each observation thanks to the observed distribution of flare fluxes and durations. We confirmed a constant overall flaring rate and a rise of the flaring rate for the faintest flares from 2014 Aug. 31 and identified a decay of the flaring rate for the brightest flares from 2013 Aug. and Nov.. A mass transfer from the Dusty S-cluster Object (DSO)/G2 to Sgr A* is not required to produce the rise of bright flaring rate since the energy saved by the decay of the number of faint flares during a long time period may be later released by several bright flares during a shorter time period.

Introduction

The closest supermassive black hole Sgr A* ($\approx 4\times10^{6}\,M_\odot$; Schödel et al. 2002, Nature, 419, 694) has a very low bolometric luminosity ($\approx 10^{36}$ erg s^{-1}; Yuan et al. 2003, ApJ, 598, 301) and, consequently, a very low mass accretion rate ($\approx 10^{-6}\,M_\odot$/yr). Above this very low luminosity, flaring activity can be observed in near-infrared, X-rays, sub-millimeter and radio.

We want to test the significance and persistence of the increase of flaring rate argued by Ponti et al. (2015) and to investigate the existence of a threshold of unabsorbed flare flux or fluence leading to any change of the unbiased flaring rate thanks to:

- additional observations performed in 2015 with Chandra and XMM-Newton;
- the overall 2006–2015 Swift campaigns;
- the improvement of the analysis methods: consistent computation of the flux from the extracted spectra and the corresponding calibration files, correction of variable PSF and vignetting due to target variable position in Swift's X-ray telescope, correction of the detection biases,...

The results of this X-ray study are reported in Mossoux & Grosso (2017, A&A, in press, arXiv: 1704.08102).

The X-ray observations

We work with the overall X-ray observations (2–10 keV) from 1999–2015 where Sgr A* was observed with an off-axis angle lower than 8′:

- XMM-Newton: 54 observations (total exposure of 2.2 Ms);
- Chandra: 121 observations (total exposure of 5.8 Ms);
- Swift: 1438 observations (total exposure of 5.8 Ms).

$\Rightarrow$ 107 X-ray flares detected.

The intrinsic flare distribution

Fluxes and durations of flares observed with XMM-Newton and Chandra (black points; $\boldsymbol{x}_i$);
Delaunay tesselation (blue triangles)

Delaunay tesselation field estimator:

$$d_{\rm obs}(\boldsymbol{x}) = d_i + \nabla d|_m\,(\boldsymbol{x}-\boldsymbol{x}_i)$$

$\rightarrow$ flare density in the convex hull

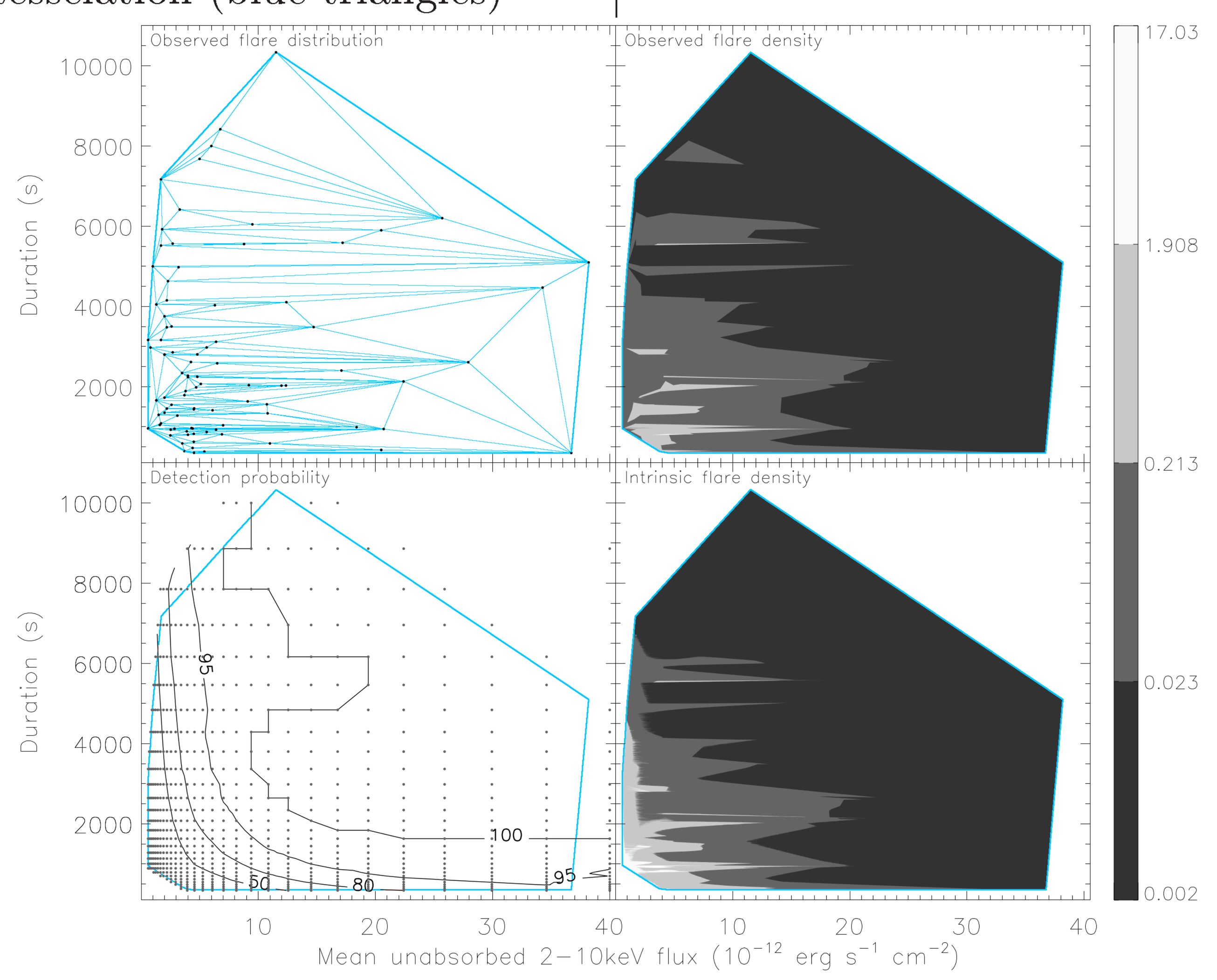

Merged detection efficiency in percent ($p_{\rm merged}$) with a false positive rate for the flare detection of 0.1% for XMM-Newton and Chandra from 1999 to 2015, obtained from simulated observations with variable exposure (500 per grid point).

The observed distribution corrected from the detection bias (Schaap & van de Weygaert 2000, A&A, 363, L29):

$$d_{\rm intr}(\boldsymbol{x}) = d_{\rm obs}(\boldsymbol{x})/p_{\rm merged}(\boldsymbol{x})$$

The unbiased X-ray flaring rate

Average flare detection efficiency: $\eta = \frac{\int\int p_{\rm obs}(\boldsymbol{x})\times d_{\rm intr}(\boldsymbol{x})\,d\boldsymbol{x}}{\int\int d_{\rm intr}(\boldsymbol{x})\,d\boldsymbol{x}} < 1$

$\Rightarrow$ Correction of each observational exposure: $T_{\rm corr} = T_{\rm obs}\times\eta$

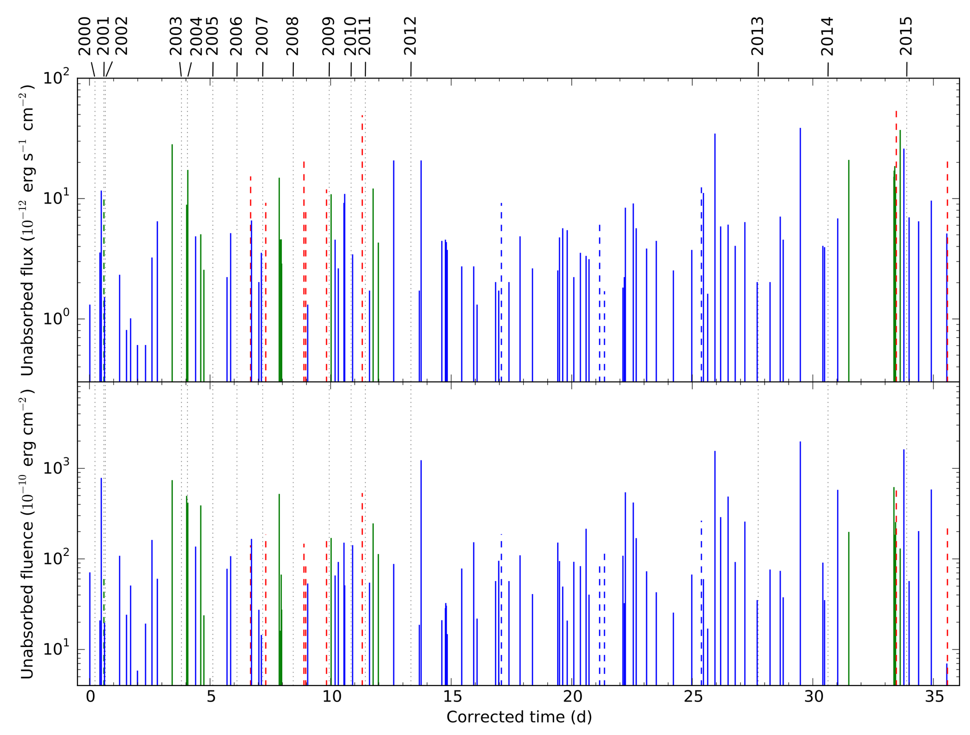

Figure 1: Temporal distribution of the flare fluxes (*Top panel*) and fluences (*Bottom panel*) corrected from the sensitivity bias and without observing gaps. The dashed lines are only lower/upper limits on the flare flux and fluence due to the truncated flare duration when it begins/ends before/after the start/end of the observation. Chandra, XMM-Newton, Swift flares.

With the Bayesian block algorithm, we determined a constant intrinsic flaring rate of 3.0±0.3 flares/day, which is higher than 1.0-1.3 flares/day of the Chandra 2012 XVP campaign (Neilsen et al. 2013, ApJ, 774, 42) since we corrected the detection bias.

Search for flux and fluence thresholds

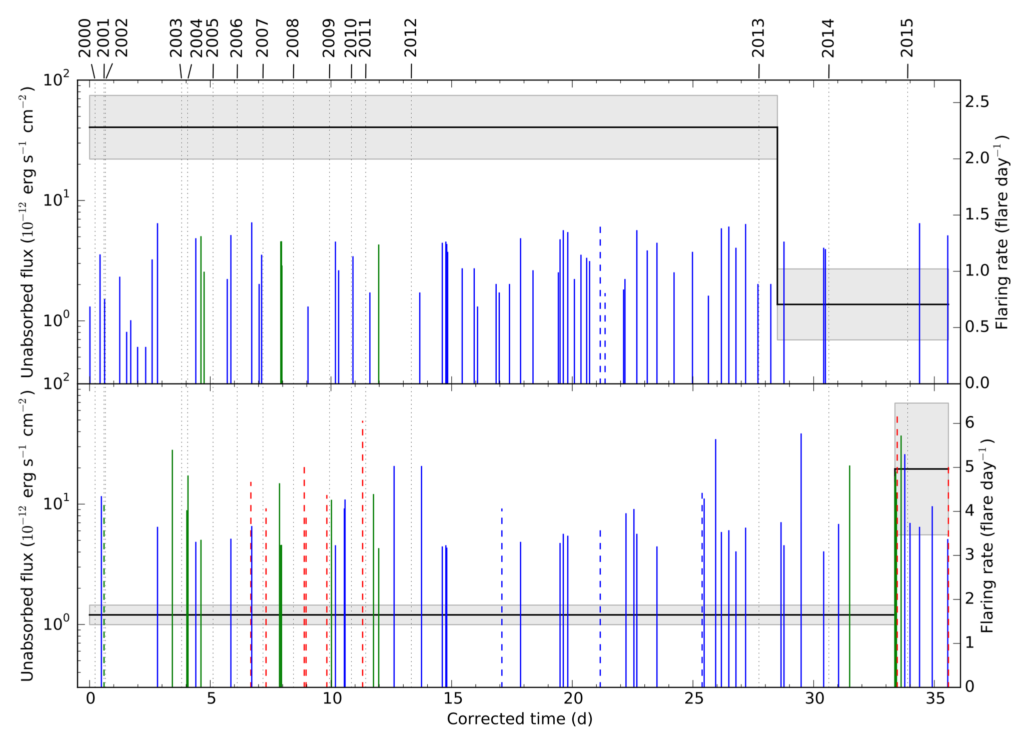

Figure 2: Search for a flux threshold leading to a change of X-ray flaring rate. The Bayesian blocks are indicated with thick black lines with the gray error bars.
Top panel: Result of the top-to-bottom search where at each step, the brightest flare was removed until a change of flaring rate was found.
Bottom panel: Result of the bottom-to-top search where at each step, the faintest flare was removed until a change of flaring rate was found.

	Flux (10^{-12} erg s^{-1} cm^{-2})	Number of flares	Corrected of the change point	Date of the change point	First block (Flare per day)	Second block (Flare per day)	Significance (%)
Top-to-bottom	< 6.5	70	28.5	2013 May 25–July 27	2.3 ± 0.3	0.7 ± 0.3	96.6
Bottom-to-top	> 4.0	66	33.4	2014 Aug. 31	1.6 ± 0.2	5.0 ± 1.5	95.2

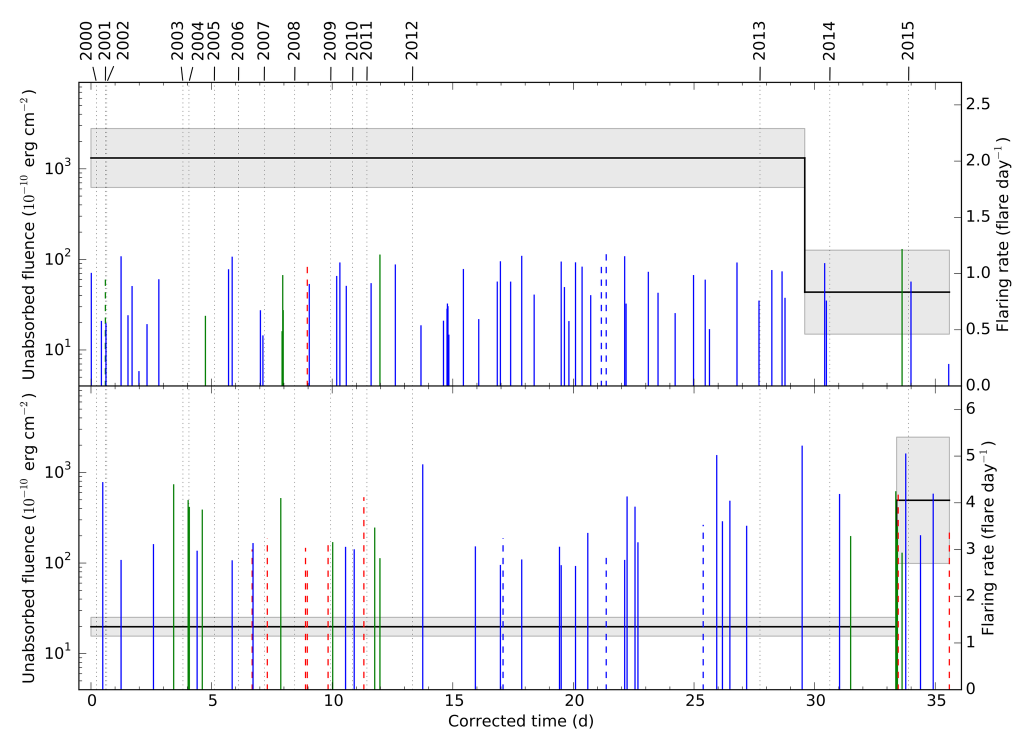

Figure 3: Search for a flux threshold leading to a change of X-ray flaring rate. The Bayesian blocks are indicated with thick black lines with the gray error bars.
Top panel: Result of the top-to-bottom search where at each step, the most energetic flare was removed until a change of flaring rate was found.
Bottom panel: Result of the bottom-to-top search where at each step, the less energetic flare was removed until a change of flaring rate was found.

	Fluence (10^{-10} erg cm^{-2})	Number of flares	Corrected of the change point	Date of the change point	First block (Flare per day)	Second block (Flare per day)	Significance (%)
Top-to-bottom	< 121.1	65	29.6	2013 July 27–Oct. 28	2.0 ± 0.3	0.8 ± 0.4	95.1
Bottom-to-top	> 91.3	54	33.4	2014 Aug. 31	1.2 ± 0.2	4.1 ± 1.3	95.1

Energy saved by the decay of the X-ray flaring rate for the less energetic flares:
$E_{\rm saved} < (9.2\pm4.8)\times10^{-8}\,{\rm erg\,cm^{-2}}$.
Energy released by the rise of the X-ray flaring rate for the most energetic flares:
$E_{\rm released} > (5.6\pm2.7)\times10^{-8}\,{\rm erg\,cm^{-2}}$
$\Rightarrow E_{\rm saved} \geq E_{\rm released}$

Conclusion

- Improved determination of the intrinsic flare distribution of Sgr A*;
- The overall X-ray flaring rate is constant;
- A decay of the faint flaring rate is detected 7 months *before* the DSO/G2 pericenter passage on 2014 Apr. 20 (Mar. 1-Jun. 10) at 2032 $R_{\rm s}$ from Sgr A* (Valencia-S. et al. 2015, ApJ, 800, 125) $\Rightarrow$ difficult to explain by the tidal disruption of the DSO/G2, whose stellar nature is now well established;
- The rise of the bright flaring rate 3 months after the DSO/G2 pericenter passage is confirmed and may be produced by the energy saved by the decay of the number of less energetic flares that we have identified $\Rightarrow$ No need of mass transfer from the young star DSO/G2 to Sgr A* to explain this rise in the bright flaring rate.